JREE: Vol. 3, No. 3, (Summer 2016) 31-43

Journal of Renewable Energy and Environment

Research Article

Journal Homepage: www.jree.ir

One-Dimensional Electrolyzer Modeling and System Sizing for Solar Hydrogen Production: an Economic Approach

Mehdi Jamali Ghahderijani, Fathollah Ommi*

Department of Mechanical Engineering, Tarbiat Modares University, Tehran, Iran

P A P E R I N F O

Paper history:
Received 03 March 2016
Accepted in revised form 04 October 2016

Keywords:
Electrolyzer
PEM
Dynamic Modeling
Hydrogen Production

A B S T R A C T

In this paper, a standalone solar based Hydrogen production in Tehran, the capital of Iran, is simulated and the cost of produced hydrogen is evaluated. Local solar power profile is obtained using TRNSYS software for a typical parking station in Tehran. The generated electricity is used to supply power to a Proton Exchange Membrane (PEM) electrolyzer for Hydrogen production. Dynamic nature of solar power and necessity of reasonable accuracy for estimating the amount of produced Hydrogen, leads to propose a new 1D dynamic fluid flow model for PEM electrolyzer cell simulation. The Hydrogen price in this system is estimated using Equivalent Annual Worth (EAW) analysis. Although it is convenient to select a yearly useful lifetime for electrolyzer as well as solar cells, in this paper, an hourly lifetime which allows finding the Hydrogen cost based on electrolyzer operating time, is considered. Also, electrolyzer sizing is done by selecting various numbers of cells for each stack and alternatives are compared from performance and economic point of view. In this regard, 4 cases consisting of 2, 3, 4, and 5 electrolyzer cells are compared. Hydrogen price at each case is evaluated and sensitivity analysis is performed. Results represent that the larger the electrolyzer sizes, the higher would be the system efficiency and consequently higher Hydrogen production would be obtained. However, the system with higher efficiency is not always an economical choice. As an alternative, turning the electrolyzer off in some conditions is also investigated for possibility of extending lifetime and reducing the Hydrogen price. It shows reduction in the efficiency for all cases though in this situation the efficiency does not necessarily increase with the electrolyzer size. It is also found that turning off the electrolyzer under specified minimum current density (2000 A/m2) in all cases, reduces the final price of the produced Hydrogen.

1. INTRODUCTION

In recent years, energy shortage and environmental impacts due to consuming fossil fuels have led to development of renewable energy systems. Among renewable energy sources, solar energy is widely accepted as the alternative to fossil fuels and Hydrogen as an effective energy carrier in the near future [1]. Water electrolysis using emission free power resources would be able to produce Hydrogen efficiently. Among all electrolyzer types, Proton Exchange Membrane (PEM) has been the subject of many researches. Higher current density tolerance, higher purity of produced gas and safer operation because it does not use harmful liquid electrolytes in comparison to other technologies, presents the PEM type as an attractive alternative. Thus, some recent studies are focused on Hydrogen production from renewable energy using PEM electrolyzer and system optimization. Ghribi et al. [2] studied a Hydrogen production system which utilized a PEM electrolysis driven by a PV solar energy in Algeria. Dursun et al. [3] modeled a stand-alone renewable hybrid power system and employed a PEM electrolyzer for Hydrogen production. Sopian et al. [4] developed a mathematical model for investigating Performance of a PV–wind hybrid system for Hydrogen production. Ahmadi et al. [5] carried out an energy and exergy analysis of Hydrogen production. In their study, a PEM electrolysis is powered by solar-boosted ocean thermal energy conversion. Optimal Hydrogen production via direct coupling of PV array and PEM electrolyzer is also investigated in some researches [6-8].

Since renewable energy sources such as solar energy are dynamic in nature, whole system should be treated dynamically. Therefore, an appropriate dynamic PEM electrolyzer model is needed to find Hydrogen production rate at a specific time interval. This model should provide adequate accuracy as well as good

*Corresponding Author's Email: fommi@modares.ac.ir (F. Ommi)

simulation speed at the same time. In the literature, there are various models with different levels of details and difficulties. Görgün [9] developed a dynamic model based on conservation of mole balance at the anode and the cathode. Dale et al. [10] presented a semi empirical model and considered a temperature dependency of reversible voltage. Santarelli et al. [11] investigated the effect of temperature, pressure, and feed water flow rate on the electrolyzer performance using a regression model. Marangio et al. [12] proposed a theoretical model of electrolyzer system consisting of activation, concentration, and ohmic over-potentials. Awasthi et al. [13] developed a dynamic model in MATLAB/Simulink with the ability to investigate the effects of different operating conditions and electrolyzer components. Lee et al. [14] represented a dynamic model of PEM electrolyzer for regenerative fuel cell applications. Kim et al. [1] developed a dynamic model of high-pressure PEM water electrolyzer. All above mentioned models are zero dimensional, exempt Kim et al. model which is one-dimensional.

Hydrogen price and its reduction, are important factors in developing the solar Hydrogen production systems. There are some researches in the literature which deal with renewable Hydrogen production and system optimization from economical point of view [15-19]. It seems that appropriate system design and sizing is simple but it is an effective way which can lead to cost reduction of Hydrogen production with the available technology.

In this paper, the power profile of the photovoltaic panels installed on a typical car parking station is considered to drive a PEM electrolyzer for hydrogen production. TRNSYS software is used for the weather data in Tehran and PV panel simulation. To simulate PEM electrolyzer behavior with good accuracy as well as reasonable run time, a new one dimensional dynamic model is proposed. The proposed model is used to evaluate dynamic behavior of a PEM electrolyzer driven by typical yearly solar power generated from photovoltaic panels which are located in Tehran. A single electrolyzer cell is modeled and with the assumption of identical cell performance, the results are extended to the whole stack. Electrolyzer sizing is done by selecting various numbers of the cells for each stack. Four cases consisting of 2, 3, 4, and 5 cells are investigated. By using Equivalent Annual Worth (EAW) analysis, the Hydrogen price is calculated and compared. Although it is convenient to select a yearly useful lifetime for electrolyzer as well as solar panels, in this paper an hourly lifetime is considered which allows finding the Hydrogen cost based on electrolyzer operating time. As an alternative at each case, the possibility of turning the electrolyzer off at below a minimum current density is also investigated. This alternative reduces operating time of electrolyzer at each year which leads to extending useful yearly life time and on the other side, declining the amount of produced Hydrogen. To find the optimum choice, the price of produced Hydrogen is calculated and compared in all cases at various minimum current densities.

2. ELECTROLYZER MODELING

Fig. 1 shows the schematic of a PEM water electrolyzer in which, the electrolyzer cell is divided into three segments namely anode channel, cathode channel and Membrane Electrode Assembly (MEA). Each segment could be split into some small and equal control volumes. At each control volume in the anode and cathode channels, fluid flow equations should be considered as well as water diffusion into/from MEA. In contrast, it is feasible to neglect these equations for MEA section without losing accuracy in the system modeling level. Beside fluid flow, the electrochemical equations should be solved at each control volume. In the following sub-sections, governing equations and solving methods are briefly explained.

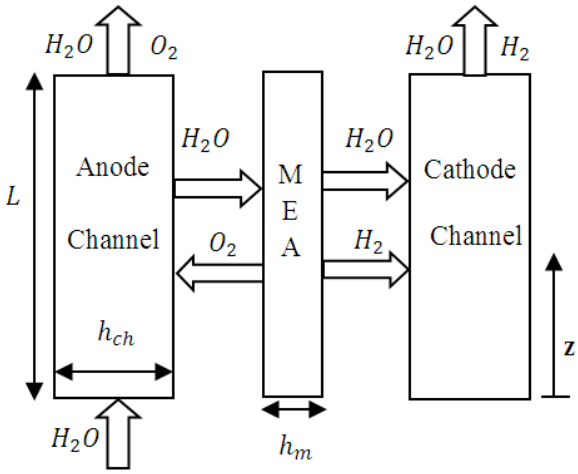

Figure 1. Schematic of a PEM electrolyzer cell

2.1. Fluid Flow in Channels

Liquid water enters into the anode channel and some of that diffuses into MEA to get into the cathode channel. In the other side, gases are produced in the electrodes and diffused to get into the channels. As a result of these phenomena, gas and liquid states exist in the channels at the same time. So, the fluid flow in the channels should be treated as a two phase flow. Here an unsteady homogenous two phase flow model is used to simulate fluid flow behavior in the channels at various dynamic situations. The mass transport phenomenon which occurred through the membrane, is considered as a source term in the governing equations [20]:

$$\frac{\partial \alpha_{gk}\rho_{gk}}{\partial t} + \frac{\partial \alpha_{gk}\rho_{gk}u_k}{\partial z} = \dot{n_{gk}} \quad (1)$$

$$\frac{\partial \alpha_{lk}\rho_{lk}}{\partial t} + \frac{\partial \alpha_{lk}\rho_{lk}u_k}{\partial z} = \dot{n_{lk}} \qquad k = a, c \quad (2)$$

$$\frac{\partial \alpha_{gk}\rho_{gk}u_k}{\partial t} + \frac{\partial \alpha_{gk}\rho_{gk}{u_k}^2}{\partial z} + \alpha_{gk}\frac{\partial P_k}{\partial z} = 0 \quad (3)$$

In the eEqs.1-3, α is the void fraction, ρ is partial density, u is flow velocity and $\dot{n}$ represents mass flow rate into/from the channel with subscripts l/g for liquid/gas and k for channel (anode a /cathode c), respectively.

2.2. Water Transport Mechanisms Three major water transport mechanisms exist in the PEM electrolyzer cell. These mechanisms can be categorized as concentration gradient, pressure gradient, and electro-osmotic drag. Among them, electro-osmotic drag plays the most important role in the water transportation [1, 12-13]. Water transport due to the concentration gradient is obtained using Fick's law [21]:

$$\dot{n}_d = D_W \frac{C_{W,a} - C_{W,c}}{h_m} \quad (4)$$

where, D_w is the water diffusion coefficient in membrane, h_m is membrane thickness, $C_{(w,c)}$ and $C_{(w,a)}$ are water concentration at cathode side and anode side, respectively. Water transport due to pressure gradient can be calculated using Darcy's law [21]:

$$\dot{n}_p = \left(\frac{K\rho_W}{\mu_W M_W}\right)\frac{P_c - P_a}{h_m} \quad (5)$$

where, K is the Darcy constant, and ρ_W and μ_W are density and dynamic viscosity of water, respectively. P_c and P_a represent pressure at cathode and anode side of the cell. Water transport in order of electro-osmotic drag is proportional to current density and is given by Eq.6 [1]:

$$\dot{n}_{eo} = n_{ed}\frac{i}{F} \quad (6)$$

The proportionality constant n_{ed} depends on pressure, temperature and current density. This constant can be calculated from semi-empirical relation introduced by Medina and Santarelli [22]:

$$n_{ed} = 0.0252P_c - 1.9073i + 0.0189T_m - 2.7892 \quad (7)$$

2.3. Electrochemical Equations The voltage required for breaking the water molecule link in the PEM cell is given by Eq.1:

$$V = E + \eta_{ohm} + \eta_{ac,a} + \eta_{ac,c} \quad (8)$$

where, V is the electrolyzer voltage. η_{ohm}, $\eta_{ac,a}$and $\eta_{ac,c}$ are ohmic, anode activation and cathode activation overpotentials, respectively. E is the open circuit voltage which can be determined by using the Nernst equation (Eq.9) [23]:

$$E = E_0 + \frac{RT_{cel}}{2F}\left[ln\left(\frac{P_{H_2}P_{O_2}^{\frac{1}{2}}}{a_{H_2O}}\right)\right] \quad (9)$$

where, E_0 is the standard potential, R is the gas universal constant, T_{cel} is the cell temperature and $a_{H_2O}$is the activity of water between anode and electrode that can be assumed equal to 1 for liquid state. The standard potential is calculated by using Eq.10 [23]:

$$E_0 = \frac{\Delta G_f}{2F} \quad (10)$$

where, ΔG_f is the Gibbs free energy of formation.
There are some overpotential voltages which increase the voltage of electrolyzer cell. In this paper, two types of overpotential including ohmic and activation (for anode and cathode), are considered. Ohmic overpotential in the PEM electrolyzer occurs due to electrical resistance of the cell against the electrical current and membrane resistance against proton migration. This over-potential can be formulated as below (Eq.11) [1]:

$$\eta_{ohm} = ir_e + h_m\frac{i}{\sigma_m} \quad (11)$$

In the Eq.11, r_e, h_m, and σ_m are cell electrical resistance, membrane thickness and conductivity of membrane, respectively. Here, it is assumed that electrodes are perfect conductors, so voltage is considered constant throughout them (1). Membrane conductivity depends on water content and temperature of membrane which can be estimated from the following practical equation (Eq.12) [12].

$$\sigma_m = [0.005139\lambda_m - 0.00326]\,exp\left[1268\left(\frac{1}{303} - \frac{1}{T_m}\right)\right] \quad (12)$$

Activation over-potential is obtained from simplified form of Butler-Volmer equation [12]:

$$\eta_{act,a} = \frac{RT_a}{2F}arcsinh\left(\frac{i}{2i_{0,a}}\right) \quad (13)$$

$$\eta_{act,c} = \frac{2RT_c}{F}arcsinh\left(\frac{i}{2i_{0,c}}\right) \quad (14)$$

F is Faraday constant, $i_{0,a}$ and $i_{0,c}$ are exchange current density at anode and cathode, respectively.
To calculate Production/destruction species rate the Faraday's law can be used:

$$\dot{n_{H_2}} = \frac{i}{2F} \quad (15)$$

$$\dot{n_{O_2}} = \frac{i}{4F} \quad (16)$$

$$\dot{n_{H_2O}} = \frac{i}{2F} \quad (17)$$

2.4. Solving Governing Equations
Governing equations introduced in the previous sections should be solved in a quick and efficient way. In this regard, at each time step first electrochemical equations are solved. Based on the output results and fluid flow conditions at previous time step, water transport is calculated. Then fluid flow equations which are a set of

nonlinear partial differential equations (Eqs.1-3) should be solved. The finite volume method with upwind differencing scheme [24] is used to discrete these equations. The obtained nonlinear algebraic equation set is implicitly solved by using Newton linearization method [25]. Although the implicit approach requires more computational effort at each time step than explicit approach, it needs less total run time than explicit approach. Actually in implicit approach, mesh and time step sizes are independent so that one can select a fewer mesh nodes as well as large time step which could lead to less computational effort to simulate the whole system [26].

2.5. Initial and Boundary Conditions

Fig. 2 shows the boundary conditions used for electrolyzer modeling. Inlet velocity can be obtained using the mass flow rate whereas outlet pressure can be calculated from vessel pressure. For void fraction, a special care must be taken. Despite the purity of input water, a small non zero value (e.g. 0.001) is assigned to void fraction to avoid zero gas pressure (see Eq.9). Initial conditions could be specified from a homogenous distribution of boundary conditions.

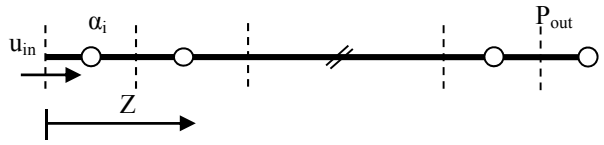

Figure 2. Boundary conditions in electrolyzer modeling

2.6. Validation

Validation of the proposed model is done considering the data extracted from Kim et al. [1] model. Table 1. summarizes the data used for the electrolyzer simulation and model validation.

TABLE 1. Parameters used in the validation process [1]

Cell dimensions: 0.3m×0.105m×0.003m
Electrode height: h_e= 0.0005m
Membrane height: h_m=0.0002 m
Number of cells: 120
Electric resistance: r_e = 0.035 mΩ
Degree of membrane humidification: λ_m =25
Anode exchange current density:$i_{0a}=10^{-6}A/m^2$
Cathode exchange current density: i_{0c}=10A/m^2
Water diffusion coefficient: $D_w=1.28\times10^{-10}m^2/s$
Darcy's constant: $K= 1.58\times10^{-18}m^2$
Nominal operating condition
Current density: i_{ave} =10000 A/ m^2
Pressure at the cathode: Pc =100 bar
Pressure at the anode: Pa = 2 bar
Inlet water flow rate: Q_{in} = 100 l/ min
Inlet water temperature: $T_{in}=55^0C$

Fig. 3 compares performance curve of Kim et al. and the proposed model in which, a good agreement is observed between two models. In Fig. 4 dynamic response to the variation of current density is presented for both models. In this regard, the average current density is suddenly changed from 1 to 1.2A/cm^2 and it is again changed to 0.8A/cm^2 at t=2 and 22min, respectively. The anode water concentration is compared at two cross sections (z=7.5 and 17.5cm) which are very close at both models.

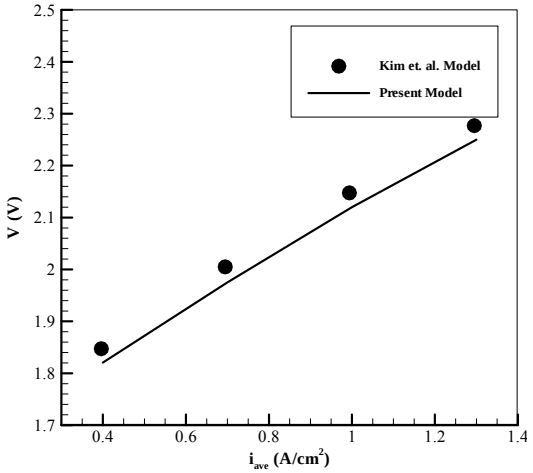

Figure 3. Electrolyzer performance curve

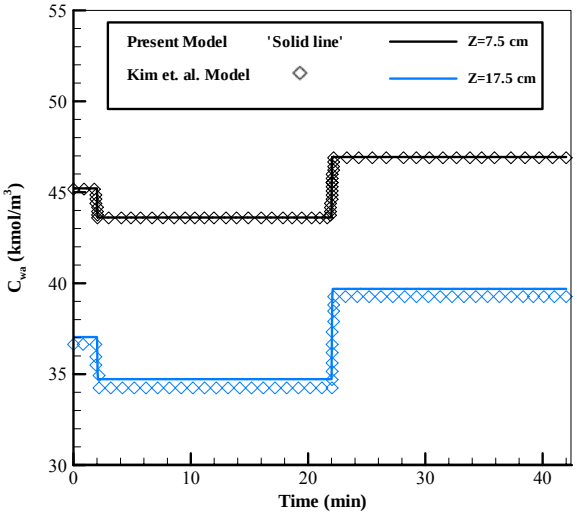

Figure 4. Dynamic response to the current density change

3. SOLAR PANEL MODELING

The solar panels are mounted at a fixed tilt angle of 35.4 which is yearly optimum tilt angle for Tehran [27]. TRNSYS software is used for the weather data and PV panel simulation. To simulate Photovoltaic (PV) cells, a primary electric model of a PV cell containing a current source and a diode, is used (see Fig. 5). Applying basic circuit laws gives the cell terminal current as follows (Eq.18):

$$I = I_{\mathrm{L}} - I_{\mathrm{D}} \tag{18}$$

Here, the light current I_L depends on the solar irradiance G and the cell temperature T_c, and is calculated according to design reference conditions (Eq.19):

$$I_{\mathrm{L}} = \left(\frac{G}{G_{\mathrm{ref}}}\right)\left(I_{\mathrm{L,ref}} + k_{\mathrm{t}}(T_{\mathrm{cell}} - T_{\mathrm{ref}})\right) \tag{19}$$

where the values of G_{ref}, $I_{\mathrm{L,ref}}$, T_{ref}, and k_{t} are given by manufacturers. The cell temperature is a function of wind speed V_{wind}, solar irradiance and ambient temperature T_0, and can be determined (in °C) with the following equation (Eq.20):

$$T_{\mathrm{cell}} = 0.943T_0 + 0.028G - 1.528V_{\mathrm{wind}} + 4.3 \tag{20}$$

which was developed by Chenni et al. [28] using experimental data from six solar cell technologies. The researchers stated that the dependency of the cell temperature on ambient temperature, solar irradiance, and wind speed is fairly independent of location.

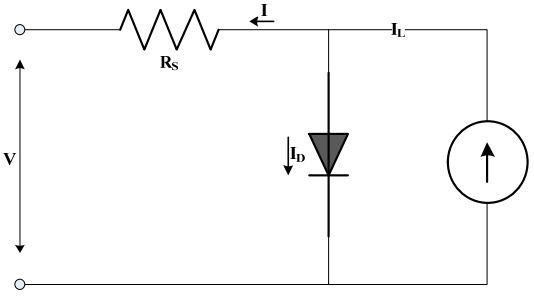

Figure 5. Equivalent circuit of a PV cell [29]

Chenni et al. [28] presented an implicit expression to calculate the maximum current I_{mp} of the PV cell:

$$I_{\mathrm{mp}} + \frac{(I_{\mathrm{mp}} - I_{\mathrm{L}} - I_0)\left[\ln\left(\frac{I_{\mathrm{L}} - I_{\mathrm{mp}}}{I_0} + 1\right) - \frac{qI_{\mathrm{mp}}R_{\mathrm{S}}}{k\gamma T_{\mathrm{ref}}}\right]}{1 + (I_{\mathrm{L}} - I_{\mathrm{mp}} + I_0)\frac{qR_{\mathrm{S}}}{k\gamma T_{\mathrm{ref}}}} = 0 \tag{21}$$

This expression can be solved using the Newton-Raphson method. At the maximum power point, the first derivation of power with respect to the voltage would be zero. Rearranging the consequent equations results in an explicit expression for the maximum voltage V_{mp} as a function of the maximum terminal current:

$$V_{\mathrm{mp}} = \frac{kT_{\mathrm{ref}}}{q}\ln\left(\frac{I_{\mathrm{L}} - I_{\mathrm{mp}}}{I_0} + 1\right) - I_{\mathrm{mp}}R_{\mathrm{s}} \tag{22}$$

The maximum current and voltage which occurs is called the maximum power point P_{mp}:

$$P_{\mathrm{mp}} = I_{\mathrm{mp}}V_{\mathrm{mp}} \tag{23}$$

4. ECONOMIC APPROACH

An economic analysis can be used to select appropriate electrolyzer sizing and working condition. The best parameter for comparison would be price of the produced Hydrogen at each case which can be calculated using EAW analysis. In EAW analysis, the annual total cost and annual total Hydrogen production should be evaluated. The cost of the plant can be divided into initial cost (consisting of equipment purchasing and installation cost) and running cost (consisting of operating and maintenance cost). The present worth (PW) of total cost during project lifetime (present cost) is calculated by Eq.24 [30]:

$$PW = FW(1+i)^{-N} \tag{24}$$

where FW is value of the net cost at Nth year and i is expected project annual interest rate. The annual cost corresponding to present cost is obtained using eq.25 [30]:

$$A = PW\frac{i(1+i)^N}{(1+i)^N - 1} \tag{25}$$

5. SIMULATION PROCEDURE

Fig. 6 shows the solving procedure flowchart of governing equations and the computer code which is developed based on the proposed model. In this regard, at first the constant parameters which are consisted of electrolyzer cell geometry (and also number of cells), fluid properties, and electrochemical constants, should be entered to the code. After performing variables initialization, the solar power obtained from solar panels can be computed using Eqs.18-23. Then electrochemical equations (Eqs. 8-14) should be solved. By solving these equations, average current density is obtained. In this step, if the average current density was less than a specified minimum current density i_{min} (see sec.6), solving process would be stopped and next iteration will be started. Otherwise, the species production/destruction rates can be determined using Eq.8-Eq.10. Thereafter, using Eqs.4-7 water transport rate which allows to calculate mass flow rate into/from the channel ($\dot{n}$) could be attained. The most difficult and time consuming step is solving the set of nonlinear partial differential equations (Eqs.1-3). Finding velocity, void fraction, and density of each species at channels allows calculating mass flow rate of Hydrogen (Eq.29). The iterations should be continued at new time step and ended when reaching the specified time (t_{max}). Then total mass of Hydrogen can be obtained by using Eq.28 and followed by economic analysis (Eqs.24-25). Reporting the results would be the final step of simulation procedure.

6. SYSTEM DEFINITION

The electricity for electrolysis is provided by three identical PV panels which are installed in series and four that are installed in parallel on the roof of a typical parking car station. The area of each panel is assumed to be 0.9 m^2 which means that the total area of solar panels is 10.8 m^2. Fig. 7 shows the power generated by solar panels during a year in Tehran.

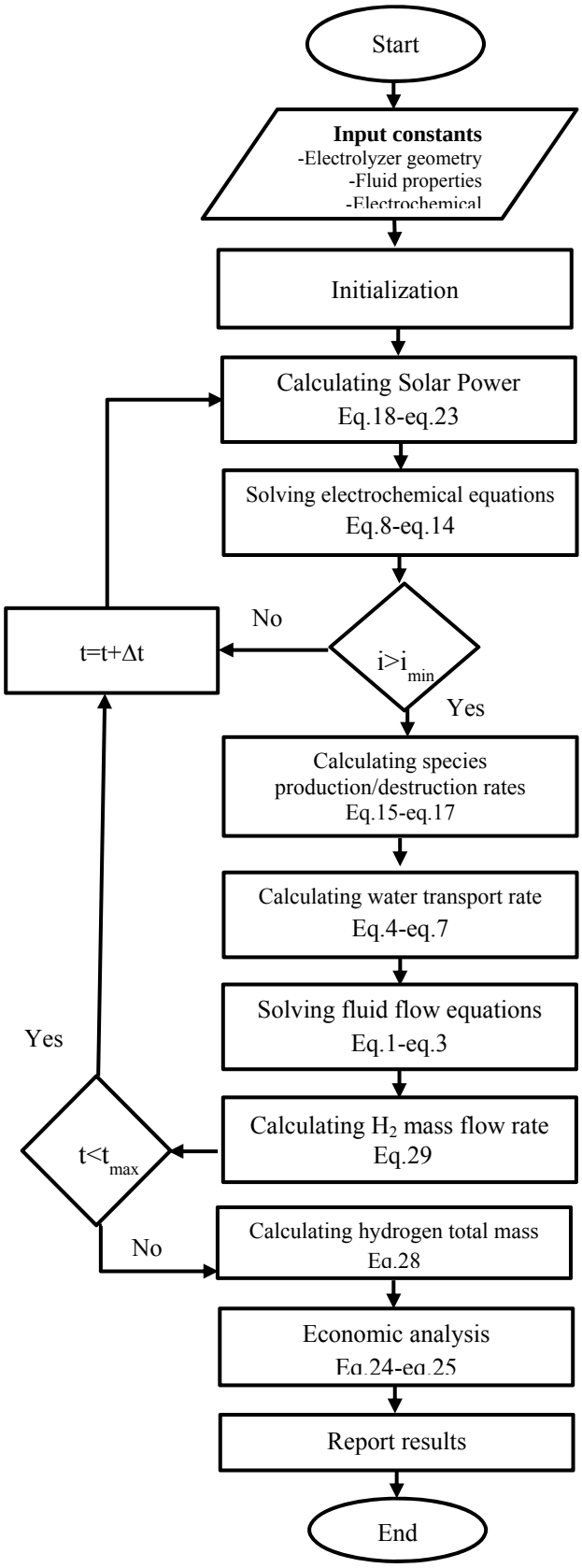

Figure 6. Flowchart of solving procedure of proposed model

As it can be expected, the solar power generation increases dramatically in hot and long days. This power is directly supplied to the PEM electrolyzer. To find suitable sizing of the electrolyzer, performance of four cases (2-cell, 3-cell, 4-cell, and 5-cell) are evaluated. It is assumed that all cells are identical and their upper limit of current density is 12000 A/m^2 while the electrolyzer pressure at each side (anode/cathode) is set to be atmospheric. The power more than maximum allowed power is considered to be lost. Electrolyzer efficiency and total system efficiency of Hydrogen production are calculated using Eqs .26-27:

$$\eta_E = \frac{HHV n_{H2}}{V i} \quad (26)$$

$$\eta_{sys} = \frac{HHV m_{H_2}}{P_t M_{H_2}} \quad (27)$$

where, HHV represents high heating value of Hydrogen, n_{H2} is Hydrogen production rate in [mol/m^2.s], m_{H2} is total mass of produced Hydrogen in [kg], M_{H_2} is hydrogen molecular mass, and P_t represents total solar energy generation. The total mass of produced hydrogen can be obtained using Eq. 28:

$$m_{H2} = \int \dot{m}_{H2} dt \quad (28)$$

where, $\dot{m}_{H2}$ is the mass flow rate of Hydrogen and can be calculated with Eq. 29:

$$\dot{m}_{H2} = \alpha_{gc} \rho_{gc} u_{gc} w_{ch,c} h_{ch,c} \quad (29)$$

As it is shown in Fig. 7, the power produced by solar panels varies from zero (in the night) to the maximum value which is different at each day. Therefore, the maximum electrolyzer capacity (current density equal to 12000 A/m^2) cannot be used at all operating time which indicates an untapped investment. On the other side, by turning off the electrolyzer when the power generation is low, the useful lifetime can be extended at the expense of losing solar power and lower hydrogen production. Consequently, a tradeoff is required to find optimum condition from economic point of view. In this regard, three various minimum current density limits (including 0, 2000, and 4000 A/m^2) are simulated and compared.

To compute the Hydrogen price, an economic analysis is done. For the PV, price of 4000 $/kW [17, 31] with lifetime of 20 years was considered and no operating cost is considered. Due to lack of mass production, there are many suggestions for the electrolyzer capital cost (1500 $/kW [17] -5000$/kW [31]). Although in most researches at system level study, the lifetime of electrolyzer is considered in year, it would be more precise to define lifetime based on operation time. In this paper three scenarios 1500, 3000, and 5000 $/kW with 36000 hours lifetime and no operating cost are investigated. The maximum power of solar panels regarding the area of a parking station is computed to be 4.2 kW, while the maximum power of each electrolyzer cell is calculated to be 775 W based on maximum allowed current density (12000A/m^2). All economic analyses are done with the interest rate equal to 6% per year.

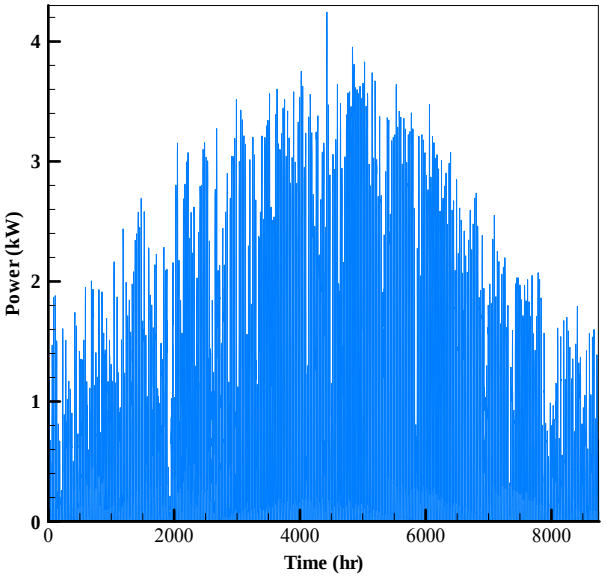

Figure 7. Solar Power generation profile during a year in Tehran

7. RESULTS AND DISCUSSION

Fig. 8 shows accumulated Hydrogen production profile for various electrolyzer sizes without any limitation on the minimum input power (i.e., I_{min}=0 A/m^2). As it can be seen, there is an insignificant difference between Case III (4-cell electrolyzer) and Case IV (5-cell electrolyzer), but variation of amount of produced Hydrogen by other alternatives is significant. In addition, the total system efficiency is raised by increasing electrolyzer cells which is as a result of higher power converting into Hydrogen (see Fig. 9). However, the same behavior of electrolyzer efficiency has a different reason. By precise inspection of the current density profile (Fig. 10), it can be seen that the average current density is going to reduce by increasing the number of electrolyzer cells. From Eqs. 11-14 it is interpreted that at higher current density the over potential would be higher which leads to reducing electrolyzer efficiency.

To improve electrolyzer lifetime, a new operating strategy is proposed. The idea is turning the electrolyzer off, when the average current density is less than a minimum allowed value. This constraint leads to utilization of higher capacity by electrolyzer while it is operating. Thus, the operating time would be reduced at the expense of lowering the Hydrogen production (see Fig. 11 and Fig. 12) and system efficiency (Fig. 13). Since the minimum required power of electrolysis rises

while number of electrolyzer cells increases, the operation time at each minimum current density is reduced in higher cell numbers. It is worth mentioning that although the operating time is reduced, the total Hydrogen production at each case with higher cell has increased except in case IV at I_{min}=4000 A/m^2. As it can be expected, turning off the electrolyzer leads to losing some of solar power. However, on the other side at some days, the solar power is higher than the total capacity of electrolyzer stack (see Fig. 14). By an increase in electrolyzer cells, this extra power can be utilized for hydrogen production. However, the minimum power for the turning on the electrolyzer is also increased. Since utilizing extra power cannot compensate the losing power due to turning off the electrolyzer, so the system efficiency is reduced in case IV at I_{min}=4000 A/m^2. So in contrast to other cases, total Hydrogen production at year and therefore total system efficiency decreases.

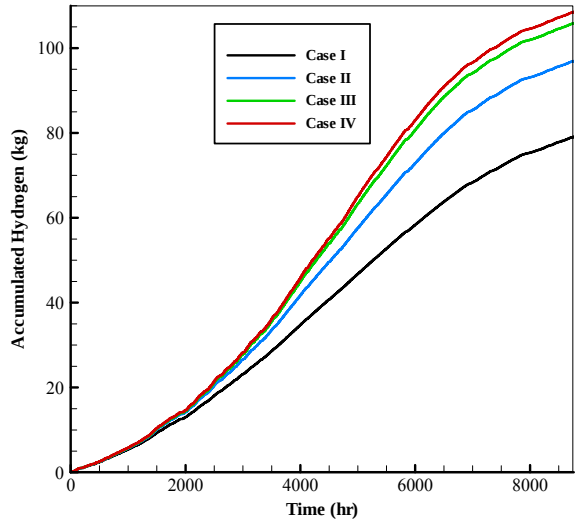

Figure 8. Accumulated Hydrogen production profile at I_{min}=0 A/m^2

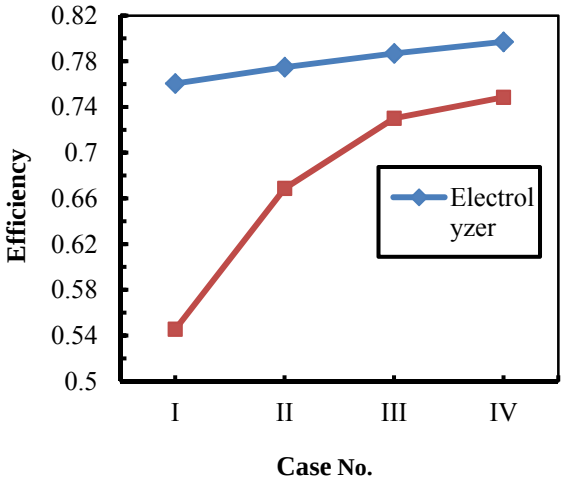

Figure 9. System and electrolyzer efficiency compression at I_{min}=0 A/m^2

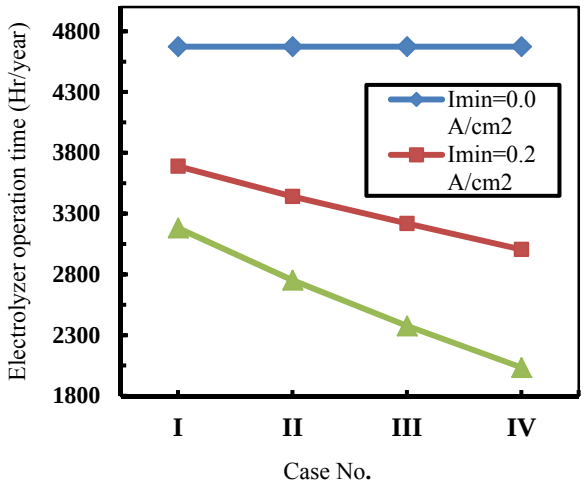

Figure 11. Electrolyzer operation time per year at various minimum current densities

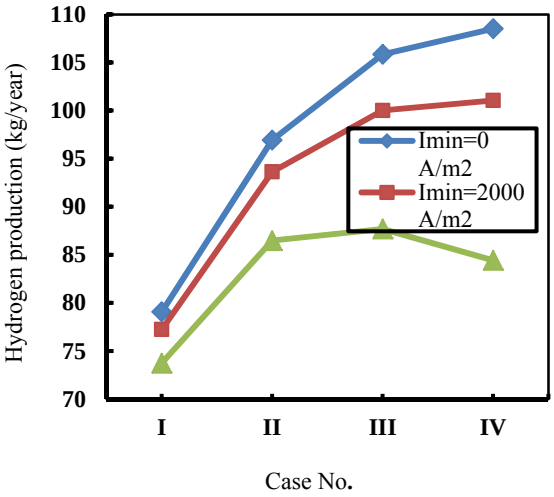

Figure 12. Hydrogen production at various minimum current densities

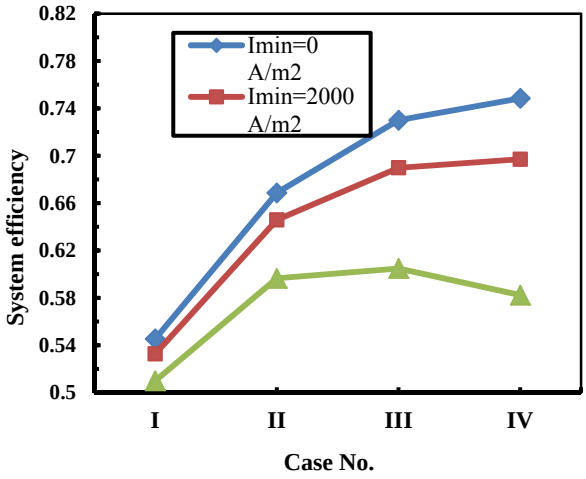

Figure 13. System efficiency at various minimum current densities

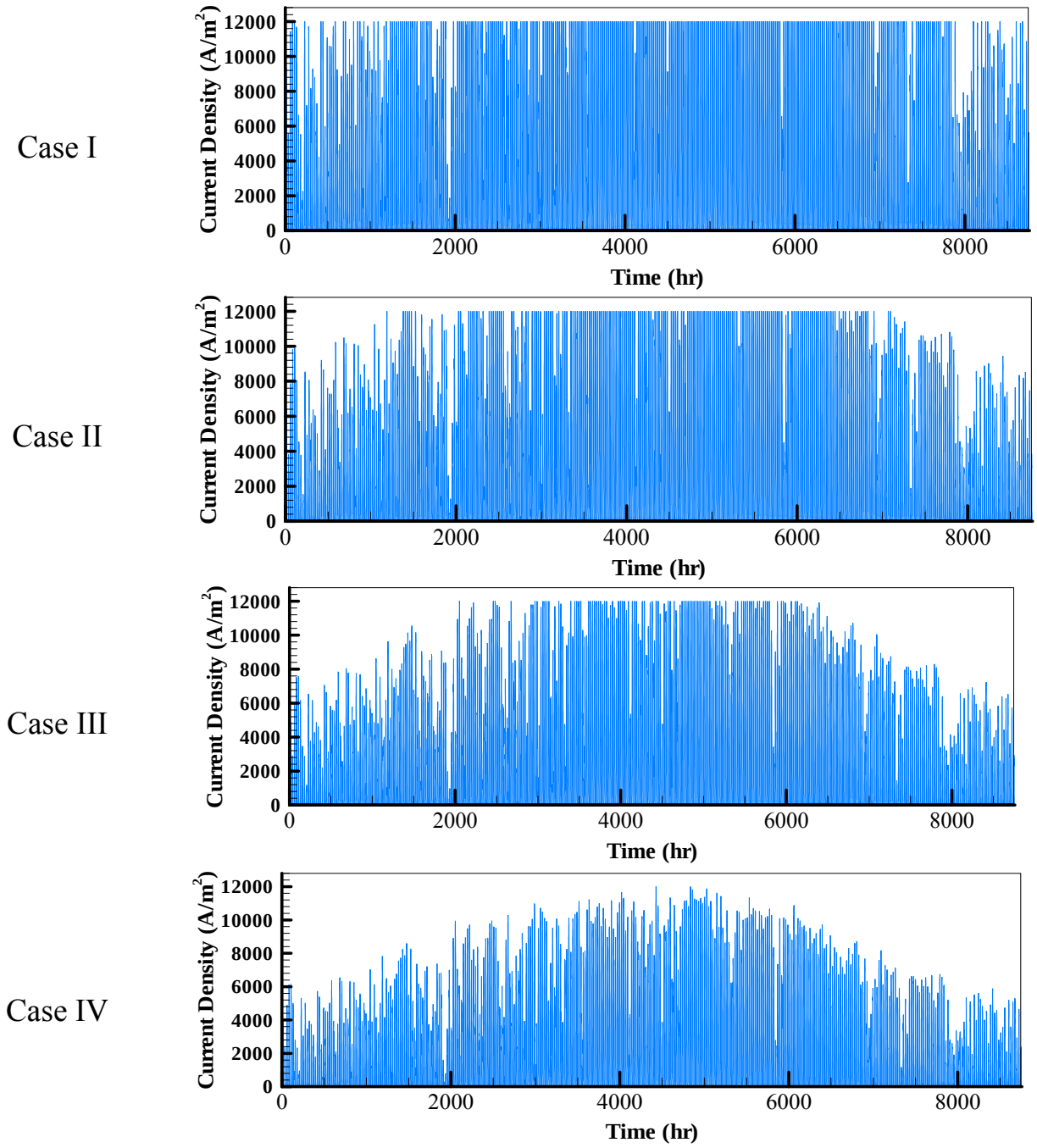

Figure 10. Average current density profile

To select the best economical choice, the hydrogen price at each case is calculated. Having system simulation done and total Hydrogen production evaluated and using EAW analysis, the annual cost of equipment at each case was estimated. By dividing the mass of produced Hydrogen at each case by its annual cost, the price of Hydrogen per mass is obtained. Fig. 15 shows the Hydrogen price for Hydrogen production without current density limitation. In this scenario, when the electrolyzer cost is not the highest one, the best choice would be case II which means a 3-cell electrolyzer. In fact, case II represents a compromising between losing less solar power and preventing high electrolyzer capital cost. Despite the lowest Hydrogen production and system efficiency in case I, when the electrolyzer capital cost is high (5000$/kW), this alternative represents lowest hydrogen price. Since the electrolyzer capital cost is the main influencer on the Hydrogen price, reducing this cost or increasing the electrolyzer lifetime can reduce the price of Hydrogen production.

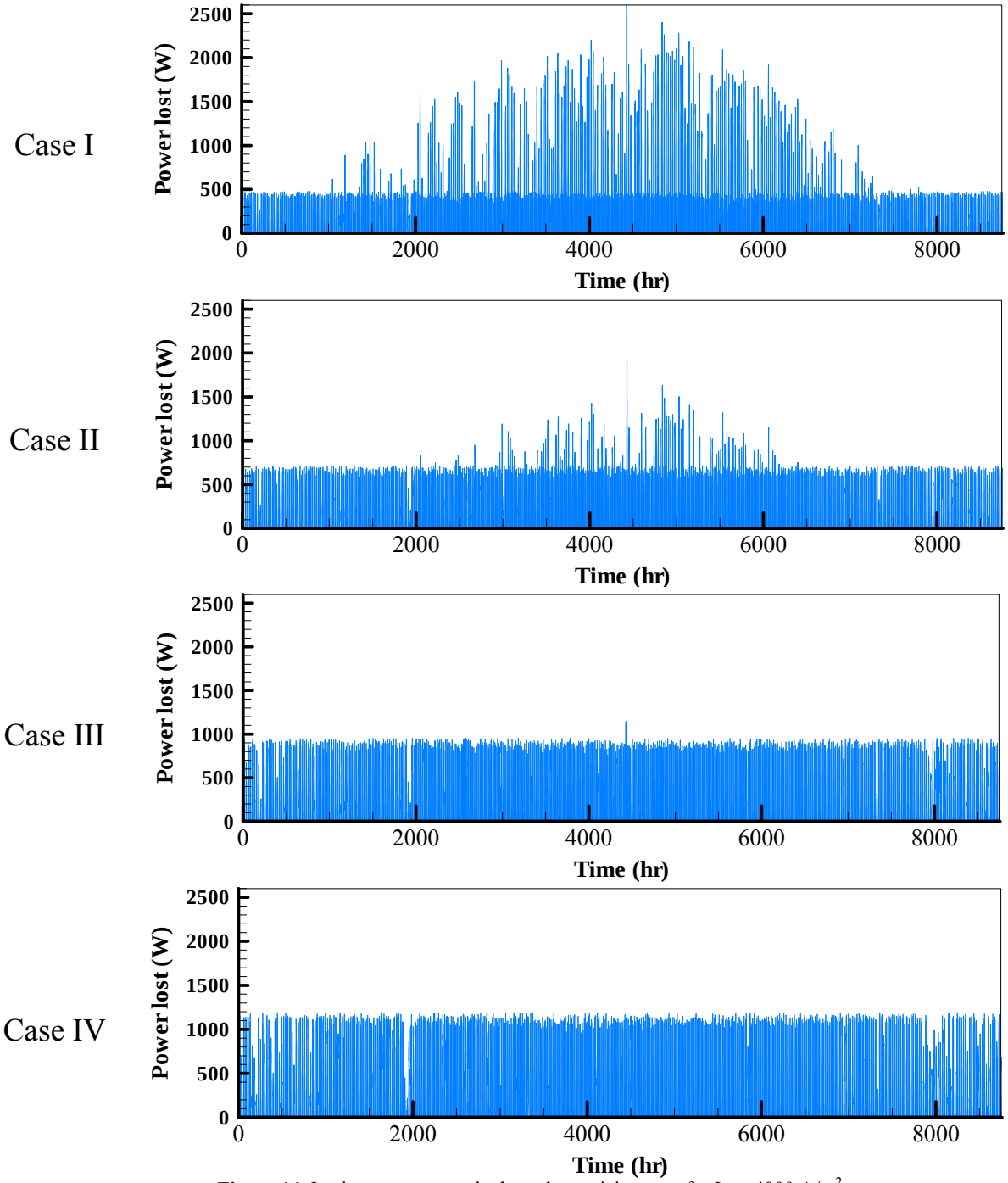

Figure 14. Losing power at each electrolyzer sizing case for I_{min}=4000 A/m^2

Fig. 16 illustrates that reducing the electrolyzer operating time results in lower hydrogen price especially when the electrolyzer capital cost is high, the system efficiency decreases (see Fig. 13). At minimum current density which equals 2000 A/m^2, the best choice is case II except at low electrolyzer capital cost (1500$/kW). Although electrolyzer turning off can increase the lifetime, reducing Hydrogen production would be the dominant parameter at high minimum current density limits. As it can be seen in Fig. 17, the Hydrogen price is raised at I_{min}=4000 A/m^2.

Table 2. summarizes the best choices for different electrolyzer capital costs. The results show that in all conditions, minimum current density which is equal to 2000 A/m^2, would be the best alternative. However, when electrolyzer capital cost is low, selecting larger electrolyzer which results higher total hydrogen production and system efficiency is preferred otherwise,

case II with 3-cell electrolyzer represents a better performance from economic point of view.

TABLE 2. Best choices at each electrolyzer capital cost

Electrolyzer cost ($/kW)	Best choice	Cell No.	I_{min} (A/m^2)	η_{sys}	Hydrogen Production(kg)	Hydrogen Price ($)
1500	Case III	4	2000	0.69	100.0	20.47
3000	Case II	3	2000	0.65	93.6	25.44
5000	Case II	3	2000	0.65	93.6	31.96

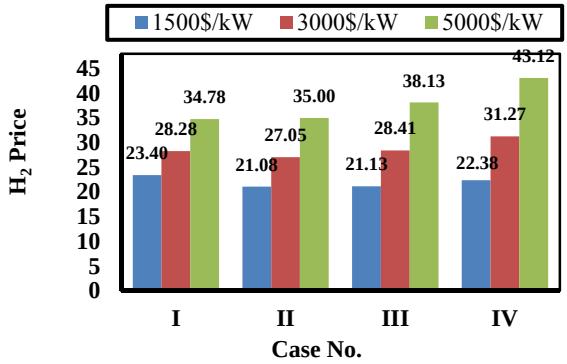

Figure 15. Hydrogen price at each electrolyzer sizing case at I_{min}=0 A/m^2

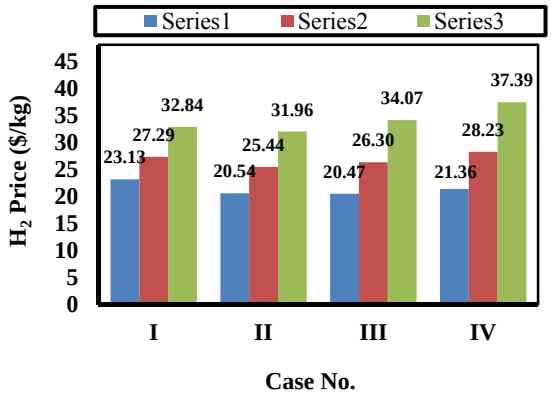

Figure 16. Hydrogen price at each electrolyzer sizing case at I_{min}=2000 A/m^2

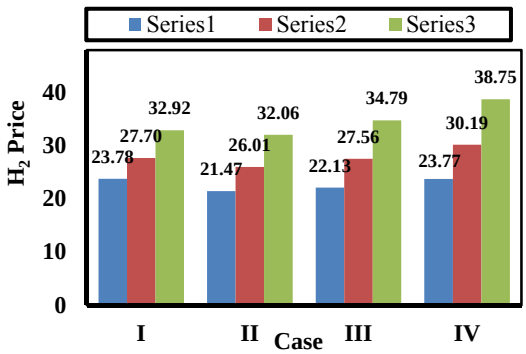

Figure 17. Hydrogen price at each electrolyzer sizing case at Imin=4000 A/m^2

4. CONCLUSION

In this paper, an appropriate system sizing was carried out by using system simulation at various sizes and operating conditions. In this regard, a new dynamic one dimensional PEM electrolyzer model was proposed which because of good accuracy and solution speed is suitable for system level simulation. The required electricity for driving the electrolyzer of a typical parking station in Tehran was considered and the power profile was obtained from TRNSYS software. Based on this solar power profile and using the proposed model, the Hydrogen production at various electrolyzer sizes was estimated. In this regard, four electrolyzers with 2, 3, 4, and 5 cells were investigated. The results showed that in the larger electrolyzer stack, system total hydrogen production at each year and the system efficiency are higher.

However, economic analysis showed that the highest system efficiency is not the best choice. Furthermore in respect to economical issues, when electrolyzer capital cost is not the highest one (in this paper 5000 $/kW) appropriate size of the electrolyzer is a 3-cell one.

To improve electrolyzer lifetime, the idea of turning it off was suggested and two scenarios (I_{min}=2000, 4000 A/m^2) were investigated. The results showed that in all cases and regardless of electrolyzer capital cost, turning off the electrolyzer under a specified minimum current density (2000 A/m^2) can reduce the produced hydrogen price though the efficiency of system is fallen down with no limitation. Moreover, when the electrolyzer capital cost is the lowest (in this paper 1500$/kW), the 4-cell electrolyzer introduces lower hydrogen price and higher efficiency, otherwise 3-cell electrolyzer is the best choice.

Nomenclature

A	Annual cost, $
a	Water activity
C	Concentration, mol m^{-3}
D	Water diffusion coefficient in membrane, m^2s^{-1}
E	Open circuit voltage, V
E_0	Standard potential, V
F	Faraday constant, 96,487 C mol^{-1}
FW	Future worth, $
G	Cell irradiance, W m^{-2}
h	Height or depth or thickness, m

I_{mp}	Maximum current, A
i	Current density, A m^{-2} or interest rate
i_0	Exchange current density, A m^{-2}
K	Darcy's constant, m^2
M	Molar mass, kg mol^{-1}
$\dot{m}$	Mass flow rate, kg s^{-1}
N	Useful lifetime, year
$\dot{n}$	Molar gas/liquid flux or generation rate, mol m^{-2} s^{-1}
n_{ed}	Electro-osmotic drag coefficient, $\mathrm{mol}_{\mathrm{H_2O}}\ \mathrm{mol}_{\mathrm{H^+}}^{-1}$
P	Pressure, bar
P_{mp}	Maximum power point, W
PW	Present Worth, $
Q	Flow rate, l min^{-1}
R	Gas universal constant, 8.3144621×10^{-5} bar K^{-1} mol^{-1}
r_e	Electrical resistance, ohm
T	Temperature, K
t	Time, s
u	Velocity, m s^{-1}
V	Cell voltage, V
V_{mp}	Maximum voltage, V
Z	Z-axis (flow direction), m

Greek letters

α	Void fraction
η	Overpotential
λ_{m}	Membrane humidification
μ	Dynamic viscosity
ρ	Density, kg m^{-3}
σ_{m}	Membrane conductivity S m^{-1}
ΔG_{f}	Gibbs free energy of formation, J/mol

Subscript

a	Anode
ac	Activation
avg	Average
c	Cathode
cel	Cell
ch	Channel
d	Diffusion
E	Electrolyzer
ed	Electro-osmotic drag coefficient
eo	Eelectro-osmosis
g	Gas
H_2	Hydrogen
H_2O	Water
in	Inlet
l	Liquid
min	Minimum
out	Outlet
O_2	Oxygen
sys	System
W	Water

REFERENCES

1. Kim, H., Park, M. and Lee, K.S., "One-dimensional dynamic modeling of a highpressure water electrolysis system for hydrogen production", ***International Journal of Hydrogen Energy,*** Vol. 38, No. 6, (2013), 2596-2609.
2. Ghribi, D., Khelifa, A., Diaf, S. and Belhamel, M., "Study of hydrogen production system by using PV solar energy and PEM electrolyser in Algeria", ***International Journal of Hydrogen Energy,*** Vol. 38, No. 20, (2013), 8480–8490.
3. Dursun, E., Acarkan, B. and Kilic, O., "Modeling of hydrogen production with a stand-alone renewable hybrid power system", ***International Journal of Hydrogen Energy,*** Vol. 37, No. 4, (2012), 3098-3107.
4. Sopian, K., Ibrahim, M.Z., Daud, W.R.W., Othman, M.Y. and Amin, N., "Performance of a PV–wind hybrid system for hydrogen production", ***Renewable Energy,*** Vol. 34, No. 8, (2009), 1973-1978.
5. Ahmadi, P., Dincer, I. and Rosen, M.A., "Energy and exergy analyses of hydrogen production via solar-boosted ocean thermal energy conversion and PEM electrolysis", ***International Journal of Hydrogen Energy,*** Vol. 38, No. 4, (2013), 1795-1805.
6. Shah, A., Mohan, V., Sheffield, J.W. and Martin, K.B., "Solar powered residential hydrogen fueling station", ***International Journal of Hydrogen Energy,*** Vol. 36, No. 20, (2011), 13132–13137.
7. Su, Z., Ding, S., Gan, Z. and Yang, X., "Optimization and sensitivity analysis of a photovoltaic-electrolyser direct-coupling system in Beijing", ***International Journal of Hydrogen Energy,*** Vol. 39, No. 14, (2014), 7202-7215.
8. Akyuz, E., Coskun, C., Oktay, Z. and Dincer, I., "Hydrogen production probability distributions for a PV-electrolyser system", ***International Journal of Hydrogen Energy,*** Vol. 36, No. 17, (2011), 11292-11299.
9. Gorgun, H., "Dynamic modeling of a proton exchangemembrane (PEM) electrolyzer", ***International Journal of Hydrogen Energy,*** Vol. 31, No. 1, (2006), 29-38.
10. Dale, N.V., Mann, M.D. and Salehfar, H., "Semiempirical model based on thermodynamic principles for determining 6 kW proton exchange membrane electrolyzer stack characterstics", ***Journal of Power Sources,*** Vol. 185, No. 2, (2008), 1348-1353.
11. Santarelli, M., Medina, P. and Cali, M., "Fitting regression model and experimental validation for a high pressure PEM electrolyzer", ***International Journal of Hydrogen Energy,*** Vol. 34, No. 6, (2009), 2519–2530.
12. Marangio, F., Santarelli, M. and Cali, M., "Theoretical model and experimental analysis of a high pressure PEM water electrolyzer for hydrogen production", ***International Journal of Hydrogen Energy,*** Vol. 34, No. 3, (2009), 2519–2530.
13. Awasthi, A., Scott, K. and Basu, S., "Dynamic modeling and simulation of a proton exchange membrane electrolyzer for hydrogen production", ***International Journal of Hydrogen Energy,*** Vol. 36, No. 22, (2011), 14779–14786.
14. Lee, B. Park, K. and Man Kim, H., "Dynamic Simulation of PEM Water Electrolysis and Comparison with Experiments", ***International Journal of Electrochemical Science,*** Vol. 8, No. 1, (2013), 235-248.
15. Ainscough, C., Peterson, D. and Miller, E. "Hydrogen Production Cost From PEM Electrolysis", DOE USA., (2014), 14004.
16. Genevieve, S., "Wind-To-Hydrogen Project: Electrolyzer Capital Cost Study", DOE USA, (2008), NREL/TP-550-44103.
17. Meratizamana, M., Monadizadeh, S. and Amidpour, M., "Simulation, economic and environmental evaluations of green solar parking (refueling station) for fuel cell vehicle", ***International Journal of Hydrogen Energy,*** Vol. 39, No. 5, (2014), 2359–2373.
18. Gökçek, M., "Hydrogen generation from small-scale wind-powered electrolysis system in different power matching

modes", ***International Journal of Hydrogen Energy,*** Vol. 35, No. 19, (2010), 10050-10059.

19. Liu, Z., Qiu, Z., Luo, Y., Mao, Z. and Wang, C., "Operation of first solar-hydrogen system in China", ***International Journal of Hydrogen Energy,*** Vol. 35, No. 7, (2008), 2762–2766.
20. Bertola, V., "Modelling and Experimentation in Two-Phase Flow", Springer-Verlag Wien GmbH, New York, (2003).
21. Bird, R.B., Stewart, W.E. and Lightfoot, E.N.,"Transport Phenomena", 2end edition, John Wiley & Sons, New York, (2007).
22. Medina, P. and Santarelli, M., "Analysis of water transport in a high pressure PEM electrolyzer", ***International Journal of Hydrogen Energy,*** Vol. 35, No. 11, (2010), 5173-5186.
23. Larminie, J. and Dicks, A. ,"Fuel cell systems explained", John Wiley & Sons, (2003).
24. Versteeg, H.K., and Malalasekera,l W.,"Introduction to Computational Fluid Dynamics: The Finite Volume Method", Pearson Education Limited, (2007).
25. Rheinboldt, W.C., "Methods for Solving Systems of Nonlinear Equations", 2end edition, SIAM, (1998).
26. Abbaspour, M., Chapman, K.S. and Glasgow, L., "Transient modeling of non-isothermal, dispersed two-phase flow in natural gas pipelines", ***Applied Mathematical Modelling,*** Vol. 34, No. 2, (2010), 495-507.
27. Jafarkazemi, F., Saadabadi, A., Pasdarshahri, H., "The optimum tilt angle for flat-plate solar collectors in Iran", ***Journal of Renewable and Sustainable Energy,*** Vol. 4, No. 1, (2012), 13118.
28. Chenni, R., Makhlouf, M., Kerbache, T. and Bouzid, A., "A detailed modeling method for photovoltaic cells", ***Energy,*** Vol. 32, No. 9, (2007), 1724-1730.
29. Ahmadi, P., Dincer, I. and Rosen, M.A., "Transient thermal performance assessment of a hybrid solar-fuel cell system in Toronto Canada", ***International Journal of Hydrogen Energy,*** Vol. 40, No. 24, (2015), 7846-7854.
30. Eschenbach, T.G., "Engineering economy applying theory to practice", Oxford University Press, New York, (2003).
31. Bezmalinovi, D., Barbir, F. and Tolj, I., "Techno-economic analysis of PEM fuel cells role in photovoltaic-based systems for the remote base stations", ***International Journal of Hydrogen Energy,*** Vol. 38, No. 1, (2013), 417-425.